Replication

Results of replicate oxidation runs on high volatile A bituminous coal (PSOC 4) show in Figure 2 that reaction rate is reproducible for the same type of coal and particle size, usually to within the experimental precision, but never exceeding a deviation of 5% for any given point. In all the figures, runs marked with a letter A were obtained with the newer apparatus; those labeled with a W are from the earlier set. Comparisons of the newer data with the similar runs from the previous operator and other gas chromatograph show somewhat greater differences, but this is probably to be attributed to the new analysis procedure. The new chromatograph is significantly more sensitive, especially in detecting the relatively smaller peaks of the carbonic gases. It is notable in Figure 2 that the replicate runs 2A and 4A from the same equipment gave results that were indistinguishable from one another. Further confirmation of reproducibility may be found in Figure 11 for runs 7A and 13A on a coal of the large pore volume group (HVC bituminous, PSOC 190).

Effect of Coal Rank

By using the carbon content of a coal sample as a convenient index of its rank, it is possible to detect trends in oxidative reactivity. One such correlation is presented in Figure 18, where the initial oxidation rates are shown for all the coals tested under the same conditions of gas flow, particle size, and temperature. Also included on the same figure is a result obtained by Kam, Hixson, and Perlmutter (1976b). It is evident that a band of values is called for, rather than a single line, but there is a discernable trend toward slower oxidation of higher rank coals. It may be noted that two replicate pairs are among the points on this figure and that their agreement is close in comparison with the scatter observed among the different coal types.

Chemical Analysis and Heating Values

Each of the coal samples was analyzed by an independent commercial laboratory to determine heating value, ultimate analysis, and proximate analysis, both before and after oxidation. Representative ultimate analysis results are summarized in Table 5.

It is clear that in general the smaller particle size samples pick up relatively larger quantities of oxygen, in agreement with the observation made by Kam, Hixson, and Perlmutter (1976c) that a coal is more readily rendered noncaking when it is oxidized in a smaller particle form, in particular when the process produces relatively more water and less of the carbonic gases. In the case of lignite (PSOC 87), however, oxygen was lost by the coal during the reaction, and the effect was greatest for the more reactive smaller size particles.

As to heating values of the several coals, the data show a strong correlation with the carbon content of a sample. Regardless of particle size, the heating value of a material changed upon oxidation primarily as the carbon changed. The results are presented in Figure 19, where a correlation coefficient of 0.86 exists for data taken with a wide range of coals of different types. There is also a suggestion in the data that generalizations regarding the fixation of oxygen that occurred for all the various bituminous coals do not apply to the lignite (PSOC 87) and the anthracite (PSOC 80) coals. The results of Table 5 show that for these coals, the most and least reactive among those tested, the result of the oxidative treatment was to increase the percent of carbon in the overall composition.

ACKNOWLEDGMENT

This research was funded by the U.S. Department of Energy (formerly ERDA, Fossil Energy Research Program) under Contract No. EX 76-S-01-2450.

NOTATION

k_4 = reaction rate constant in KHP model, hr^{-1}
R = oxygen reaction rate, g/hr/kg coal
R_i = long time asymptotic value of reaction rate
R_o = zero time intercept of reaction rate curve
t = time, hr

LITERATURE CITED

Gan, H., S. P. Nandi, and P. L. Walker, Jr., "Nature of the Porosity in American Coals," *Fuel*, **51**, 272 (1972).

Kam, A. Y., A. N. Hixson, and D. D. Perlmutter, "The Oxidation of Bituminous Coal, Part 1: "Development of a Mathematical Model," *Chem. Eng. Sci.*, 31, 815 (1976*a*).

————, "The Oxidation of Bituminous Coal, Part 2: "Experimental Kinetics and Interpretation," *ibid.*, 821 (1976*b*).

————, "The Oxidation of Bituminous Coal, Part 3: Effect on Caking Properties," *Ind. Eng. Chem. Process Design Develop.*, **15**, No. 3, 416 (1976*c*).

Manuscript received July 12, 1978; revision received January 29, and accepted February 20, 1979.

Criteria for Selective Path Promotion in Electrochemical Reaction Sequences

An analysis of consecutive electrochemical reactions is presented with some emphasis on organic electrocatalytic sequences. The effect of potential and electrode kinetic parameters on reaction selectivity and on current and rate distribution is examined in two model electrochemical reactors with channel flow or with complete mixing. Results and some examples demonstrate that the electrolyte potential is the most significant parameter for selectivity control of complex series reactions in electrochemical processing or energy generation. Criteria developed for selectivity and current or rate variation provide the basis for the design of electrochemical reactors and for optimal operation considerations with multiple electrode reactions. Such criteria and analyses apply to a number of working electrode configurations operating with ionic as well as molecular reactants.

GEORGE P. SAKELLAROPOULOS

Department of Chemical and Environmental Engineering
Rensselaer Polytechnic Institute
Troy, New York 12181

SCOPE

The feasibility of electrochemical processes for chemical production and energy generation depends on the rational choice of operating conditions and of reactor designs to promote desirable reaction paths. Reluctance to adopt electrochemical systems often stems from inadequate understanding of the combined effects of an electric field and of kinetic and mixing processes in flow reactors on the specificity of multiple electrochemical reactions. Here we present an analysis of these effects for consecutive electrochemical reactions involving one or more complex or elementary electron-transfer steps. Such reaction sequences of arbitrary kinetics for each step are commonly encountered in organic electrocatalytic and in ionic electrochemical processes.

Previous analyses of series reactions in an electric field examined a simple, mechanistic sequence involving only a slow homogeneous (nonelectrochemical) step and slow mass transfer (Sioda, 1974; Alkire and Gould, 1977), or ionic reactions lumped into one overall rate expression (Ateya and Austin, 1977). Because of their specific nature, these studies did not address any general criteria for selectivity control or for rate and current distribution with arbitrary reactions. Analyses of competing multiple reactions in flow reactors (Sakellaropoulos and Francis, 1979*a*, *b*) and at rotating disk electrodes (White and Newman, 1977; White et al., 1977) amplify the need for such criteria, for the selection of appropriate electrochemical reactor designs and of operating conditions, depending on electrode kinetics.

In the present analysis of consecutive electrodic reactions, two model electrochemical reactors are considered with channel plug flow (CER) or with complete mixing (MER) of the reacting fluid stream. By neglecting dispersive mixing and ohmic losses, the sensitivity of product yield, of rate distribution, and of energy needs to electrode kinetic and system parameters can be identified. These results lay the groundwork for further optimization considerations of electrochemical reactor cells. Of course, the design and optimization of electrochemical reactors is based on the assumption of known electrode kinetics. However, few complex electrocatalytic reactions are well characterized in the kinetic regime. The derived equations should assist in obtaining the needed transfer coefficients and other kinetic parameters of multiple electrochemical reaction schemes.

CONCLUSIONS AND SIGNIFICANCE

The selectivity of consecutive electrochemical reactions depends mainly upon the effect of electrode potential on the rate of each step and upon the retention time of reactants and products in the electric field of the reactor. The electrode potential does not play the simple role of a modifier of the rate constant ratio for two steps but becomes an important optimization parameter. Thus, the selectivity and yield of a reaction intermediate can improve in short space times and low potentials, depending on transfer coefficients, contrary to conventional kinetics.

With kinetic parameters favoring the second reaction step, high intermediate yields are expected at low anodic or positive cathodic potentials. Such potentials are often neglected in conventional electrochemical studies, but they are easily attained in electrogenerative catalytic reactors. In this case, a flow reactor can be designed with an optimal potential sequence to maximize yield.

Concentration and mixing effects on electrodic selectivity are similar to conventional reactors. High reactant conversion and promotion of mixing lower the selectivity of the reaction intermediate. However, these as well as temperature effects can be offset or even reversed by potential control.

The reaction rate and current distribution in a CER determine the electric energy requirements for electrolytic reactors or the energy capabilities of electrogenerative and fuel cells. The total average current density can be larger or smaller than the initial (maximum) current density of the first step depending on the potential and the kinetic parameters of each step. The criteria established here permit prediction of kinetic current densities attainable at given potentials and space times. In energy generation, complete reaction of the intermediate at high reactant conversions per pass may lead to an apparent limiting or declining average current density due to concentration and thence rate decrease. Such experimental limiting behavior was previously attributed to slow mass transport or electrode passivation.

Large concentration variations along a channel flow electrochemical reactor result in nonuniform local current distribution that may promote electrode or catalyst deterioration. Uniform currents can be achieved in a mixed electrochemical reactor at the expense of size. This uniform rate and selectivity and simple solution of the pertinent transport equations make the mixed reactor ideal for the needed kinetic analyses of multiple reactions.

The discussed models and the presented criteria permit a rational approach to the design and optimization of size, yield, and energy use or generation of electrochemical reactors for multiple reaction sequences. This analysis is applicable to dissolved or gas phase organic reactants as well as to ionic species, for various electrode configurations, including thin flow by porous or thin gap or slurry electrodes. Since solution of the convective transport equations for simple-order reactions (zero, one) gives similar results, discussion focuses primarily on two successive first-order steps. The qualitative predictions, however, apply equally well to other kinetic expressions and to consecutive reactions with more than two steps.

Electrochemical oxidations and reductions of neutral organic or ionic reactants often proceed via several successive steps. In the presence of an electric field, some of these steps involve electron transfer and possibly chemical and catalytic reactions. Successful promotion or inhibition of certain steps, then, can provide an incentive for the development and application of a new process. Presently, several selective electrochemical reactions are being examined for industrial use or pollution abatement (Fitzjohn, 1975; Ibl and Selvig, 1970; Newman and Tiedemann, 1975; Sakellaropoulos and Langer, 1976*a*; Weinberg, 1978). However, despite recognition of the effect of potential and electrode material on selec-

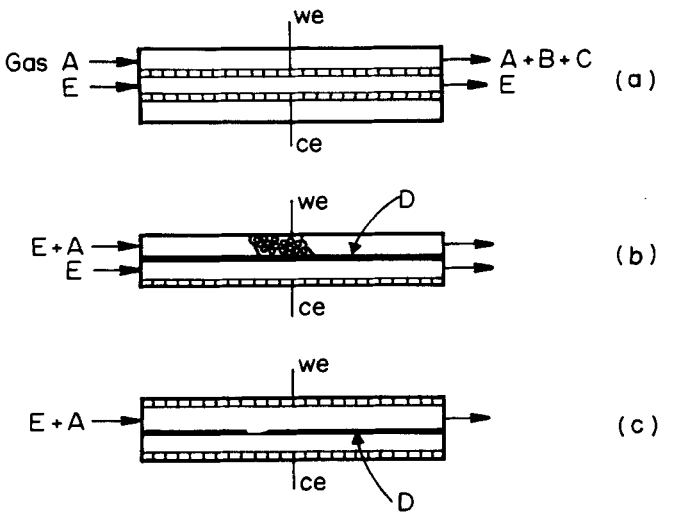

Fig. 1. Typical channel flow electrochemical reactors (CER). (a) CER for gaseous reactants; (b) CER with a thin, conductive packed bed; (c) a divided CER for dissolved reactants. D: diaphragm; E: electrolyte; ce: counterelectrode; we: working electrode.

tivity control, little information exists on a priori selection of optimal operating conditions and on criteria for the design of electrochemical reactors for multiple reactions. In particular, the advent of electrocatalytic and electrogenerative concepts (Langer and Landi, 1963; Sakellaropoulos and Langer, 1976*a*) has made electroorganic reactions possible in previously unexplored potential regions. The conditions for which such unconventional potentials are advantageous for selectivity improvement are not currently established.

Consecutive electrochemical reactions were examined by Alkire and Gould (1976) for the modeling of packed-bed, noncatalytic electrodes in the presence of slow mass transport and axial mixing. Only an elementary, first-order reaction sequence was discussed with a slow homogeneous, nonelectrochemical step (ECE mechanism). Thus, the effect of potential on selectivity and rate distribution was not explored for this or other electrochemical reactions in series. Sioda (1974) considered conventional elementary electrochemical sequences involving combinations of chemical and electron transfer steps of first order. However, analysis was restricted to a flow reactor operation at a limiting current, for which electrode kinetics and potential play no role. First-order electrochemical reactions in series were examined by Ateya and Austin (1977) in the kinetic regime for the modeling of flow through, noncatalytic electrodes. By lumping all reaction rates in one current density (rate) term, the effect of potential on the selectivity of each step was neglected, and only average current density potential results were presented.

A similar approach has also been taken in other studies of multiple reactions in closed cells (Bard and Mayell, 1962; Geske and Bard, 1959) or cells of uniform concentration (Gileadi and Srinivasan, 1964; McIntyre, 1969; Parsons, 1968). Analyses were limited to the prediction of experimentally observed apparent Tafel slopes, transfer coefficients, and fractional coulombic numbers with multiple, first-order reactions. The effects of potential, conversion, convective transport, or mixing on selectivity were not considered.

In this investigation, we evaluate these effects using two simple model electrochemical reactors. The same models proved useful in the analysis of multiple parallel reactions (Sakellaropoulos and Francis, 1979*a, b*). Thus, for complex electroorganic reactions, usually involving series as well as parallel steps, criteria from both studies can be coupled for the design and optimization of new electrochemical processes.

Idealized model reactors similar to those considered here have also been discussed by Pickett (1977), primarily for single, mass transport controlled reactions. Operation at transport limited currents would, of course, provide minimum reactor volume for single as well as multiple reactions. However, the potentials reached under these conditions can be detrimental to product selectivity in multipath reaction schemes. For instance, stepwise electrocatalytic reduction of substituted alkenes yields high selectivity for the desirable intermediate olefins at positive, electrogenerative potentials (+0.2 V), well away from the cell limiting currents (Sakellaropoulos and Langer, 1976*b*). The latter are reached only with some reactants and at potentials below 0V vs. a hydrogen electrode in the same electrolyte, conditions favoring unwanted alkane formation. For such reactions, operation in the electrode-kinetic regime is essential to avoid undesirable products and subsequent expensive separations.

Because of the central role of potential and concentration in the specificity of multipath electroorganic reactions (Sakellaropoulos and Langer, 1976*b*; Sakellaropoulos and Francis, 1976*b*) we address here electrochemical reaction sequences only under kinetic control. Although diffusive and migrative transport processes (laterally, axially, or in the pores of the electrocatalysts) would alter somewhat the intrinsic selectivity, such effects will be considered separately for our model reactors, after the basic criteria for optimal design and operation are established in this work.

THEORETICAL DEVELOPMENT

A channel flow electrochemical reactor (CER) consists of a two-electrode cell with fluid flow normal to current or charge flow. Figure 1 shows various CER's with the working electrode being a smooth metal or a thin porous matrix (a), or a thin packed-bed electrode containing microporous conductive particles (b). The electrode reaction takes place at the solid electrolyte interface between ionic and organic molecular species.

For a multiple electrochemical reaction scheme, the overall stoichiometric equations are given by Equation (1):

$$\sum_{j=1}^{S} \nu_{kj} A_j + n_k e = 0 \quad (k = 1, 2, \ldots R) \tag{1}$$

If we assume a general kinetic scheme with possible adsorption and reversible reaction, the local surface reaction rate $\bar{r}_k(z)$ and current density $\bar{i}_k(z)$ of each path is given by (Sakellaropoulos, 1977; Sakellaropoulos and Francis, 1976*b*)

$$\bar{i}_k = n_k F \bar{r}_k = n_k F \left\{ \frac{k^o_{kf} \prod_j C_j^{a_{kj}}}{\left(1 + \sum_{j=1}^{S} K_j C_j\right)^m} \exp\left[-\frac{\alpha_k FE}{\mathcal{R}T}\right] - \frac{k^o_{kb} \prod_j C_j^{b_{kj}}}{\left(1 + \sum_{j=1}^{S} K_j C_j\right)^p} \exp\left[\frac{\alpha_k' FE}{\mathcal{R}T}\right] \right\} \tag{2}$$

Here E is the working electrode potential vs. a reference electrode, the normal hydrogen electrode (NHE), and K_j are adsorption equilibrium constants. The latter are exponential functions of the electrode potential vs. the same reference for electrosorption (Bockris and Srinivasan, 1969) but do not depend on potential for molecules adsorbing without simultaneous electron transfer. The exponents m and p express the number of catalytic sites participating in each reaction. The intrinsic reaction orders a_{kj}, b_{kj} generally do not coincide with the stoichiometric coefficients ν_{kj}. The choice of a potential instead of an overpotential (which is often preferred in the electrochemical literature) is due to the lack of knowledge of reversible potentials for many complex organic reactions (Sakellaropoulos and Langer, 1976*b*).

The working electrode potential is constant for smooth electrodes, but it may vary with distance from the surface in porous electrodes owing to current flow. Such variation is given by Ohm's law and is relatively small, of the order of 5 to 10 mV, with strong aqueous electrolytes and thin, conductive porous electrodes (Austin, 1967; Pshenichnikov et al., 1972; Sakellaropoulos and Langer, 1978). With thick porous structures, however, such as packed beds, ohmic losses within the electrode could be appreciable. Here we examine the operation of smooth and thin porous electrodes with high conductivity electrolytes and negligible potential variations in the pores. This approach permits not only simple reactor analysis but also explicit identification of the role of potential on selectivity control. In addition, it allows a qualitative a priori evaluation of the effect of potential change in porous electrodes on specificity, as discussed later.

The general Equation (2) can often be simplified or approximated by simple-order reversible or irreversible kinetics. Reversible reactions are usually encountered with some metal ion or other ionic reactions. Organic electrocatalytic reactions are usually simple-order irreversible, despite possible adsorption and existence of some reversible elementary steps (Langer and Sakellaropoulos, 1975; Sakellaropoulos and Langer, 1978). In the case of a chemical path in an electroorganic reaction sequence, the kinetic term in the brackets in Equation (2) still holds, with the transfer coefficients α_k and α_k' both equal to zero. Of course, in this case no current is associated with the reaction rate ($n_k = 0$). For all electrochemical steps, the net total current density at any point along the electrode is

$$\bar{i}_t(z) = \sum_{k=1}^{R} \bar{i}_k = \sum_{k=1}^{R} n_k F \bar{r}_k \tag{3}$$

The concentration, rate, and selectivity distributions in the reactor, under steady state isothermal, potentiostatic (E = constant) operation, are obtained from the convective transport equations for independent species (Sakellaropoulos and Francis, 1979*b*):

$$-\bar{v}\cdot\nabla C_{j\infty} + \nabla\cdot D_j \nabla C_{j\infty} + \rho_b S_g (1-\epsilon) \sum_{k=1}^{R} \nu_{kj} \bar{r}_{k\infty} = 0 \tag{4}$$

In the following analysis, unidirectional channel flow is considered with uniform bulk composition normal to flow (plug flow). Axial dispersion effects are neglected in order to place an upper bound to reactor performance. Thus, results are applicable to ideal plug flow in long reactors, for which $L/D_c > 50$ (Kramers and Westerterp, 1963). Axial dispersion was considered by Trainham and Newman (1977), Ateya and Austin (1977), and Alkire and Gould (1976) (with simplified boundary conditions) for first-order ionic reactions in short, flow through electrodes at low flow rates.

In contrast to a CER, concentration and rate (current density) are uniform in a thoroughly mixed electrochemical reactor (MER) (Sakellaropoulos and Francis, 1979*a*). The convective transport equation for species j becomes, then

$$C_{jo} - C_{j\infty} + \rho_b S_g (1-\epsilon)\tau \sum_{k=1}^{R} \nu_{kj} \bar{r}_{k\infty} = 0 \quad (j = 1, 2, \ldots S) \tag{5}$$

The control volume of a MER includes the total catalyst surface and the space of the flow vessel. Here, the performance of a MER is examined to place a lower bound to selectivity and yield due to mixing. Other mixing effects, such as recycling in a CER, axial dispersion, etc., will give results intermediate between a MER and a CER.

Equations (4) and (5) apply directly to electrode reactions with reactants and products dissolved in the electrolyte. The same equations apply to the gas phase convective transport and reaction of gaseous reactants that are in local equilibrium with the electrolyte. Such gas-catalyst-electrolyte reactions are often encountered in fuel cells (Bockris et al., 1965; Vielstich, 1970) and in electrogenerative processing (Goodridge and King, 1970; Langer and Landi, 1963; Sakellaropoulos and Langer, 1976*a*). In this case, C_{jo} and $C_{j\infty}$ are the gas phase concentrations, while $\bar{r}_{k\infty}$ is evaluated at the liquid concentration $C_{j(l)}$ of each species (Sakellaropoulos and Francis, 1979*a, b*). With sparingly soluble organic reactants, the latter can be estimated from Henry's law, $C_{j(l)} = K_H \mathcal{R} T C_{j(g)}$.

The yield of a desirable product in the reaction sequence and the generated or consumed current by each reactor are obtained below by solving Equations (1) to (4) or (1) to (3), (5) with appropriate boundary conditions. Although results are illustrated for simple-order irreversible reactions, the general qualitative behavior applies also to other kinetic schemes. However, with some complex nonlinear kinetics, only numerical solutions can be obtained.

RESULTS AND DISCUSSION

Channel Flow Electrochemical Reactors

Selectivity Analysis. Consider two simple-order, irreversible electrochemical reductions in series, with dissolved reactants

$$A \xrightarrow[+e]{1} B \xrightarrow[+e]{2} C \tag{6}$$

For such reactions, the last term of Equation (2) is zero. In addition, the adsorption equilibrium terms in Equation (2) are either negligible compared to unity to give $a_{kj} > 0$ or one term is much larger than all others to give negative orders ($a_{kj} < 0$). Either behavior is not uncommon with complex organic, catalytic reactions as explained earlier. If each reaction step depends for simplicity on the concentration of one reactant, the convective transport Equation (4) yields in dimensionless form

$$\frac{dC_{A\infty}^*}{dz^*} + \lambda C_{A\infty}^{*a11} e^{-\alpha_1 \theta} = 0 \tag{7}$$

$$\frac{dC_{B\infty}^*}{dz^*} - \lambda C_{A\infty}^{*a11} e^{-\alpha_1\theta}\{1 - \mu C_{A\infty}^{*-a11} C_{B\infty}^{*b22} e^{-(\alpha_2 - \alpha_1)\theta}\} = 0 \tag{8}$$

TABLE 1. INVESTIGATED RANGE OF PARAMETERS FOR BOTH CER AND MER

Parameter	Range
Reaction orders	0, 1
Transfer coefficients	0-2
μ	$10^{-4} - 10^{4}$
λ or λz^*	$10^{-8} - 10^{5}$
θ	$(-20) - (+30)$
Potential, E(V)	$(-0.51) - (+0.77)$
Rate constant, k_1^o ($cm^{-1}\,s^{-1}$)	$10^{-8} - 10^{5}$
Reactant concentration, C_{Ao}(mole/cm^3)	$10^{-6} - 10^{-3}$

$$\frac{dC^*_{C\infty}}{dz^*} - \mu\lambda C^{*b22}_{B\infty} e^{-\alpha_2\theta} = 0 \qquad (9)$$

with initial conditions

$$z^* = 0 \quad C^*_{A\infty} = 1 \quad C^*_{B\infty} = C^*_{C\infty} = 0 \qquad (10)$$

Here λ is a dimensionless space time at zero potential vs. our reference NHE, μ is a selectivity parameter for C at zero potential, and θ a dimensionless potential

$$\lambda = \rho_b S_g (1-\epsilon) k_1^o \tau C_{Ao}^{a11-1}$$
$$\mu = \frac{k_2^o}{k_1^o} C_{Ao}^{b22-a11} \qquad (11)$$
$$C^*_{j\infty} = C_{j\infty}/C_{Ao}, \quad z^* = z/L, \quad \theta = \frac{FE}{\mathcal{R}T} \quad \tau = \frac{L}{v_z}$$

Of course, $C^*_{C\infty}$ can be also obtained from stoichiometry $C^*_{C\infty} = 1 - C^*_{A\infty} - C^*_{B\infty}$. The rate constants k^o_1, k^o_2 may be functions of concentrations of reactants in excess, for example, H^+ ions for reductions. Their magnitude (and thus that of λ and μ) depends on the choice of the reference electrode potential. Here, the universal zero potential reference of the normal hydrogen electrode has been adopted. Table 1 gives the range of changes in kinetic parameters investigated in this work.

Solution of Equations (7), (8), and (10) yields the concentrations of all species in the reactor, which are now dependent upon the electrode potential. With first-order reactions

$$C^*_{A\infty} = \exp[-\lambda z^* e^{-\alpha_1\theta}] \qquad (12)$$

$$C^*_{B\infty} = \frac{1}{\mu e^{-(\alpha_2-\alpha_1)\theta} - 1}\left[\exp(-\lambda z^* e^{-\alpha_1\theta}) - \exp(-\mu\lambda z^* e^{-\alpha_2\theta})\right] \qquad (13)$$

For some other orders or for $\mu e^{-(\alpha_2-\alpha_1)\theta} = 1$, Table 2 gives expressions for the intermediate concentration. We wish to note here that Equations (7) to (9) and (12) and (13) and the results obtained below for a CER are also applicable to a batch electrochemical cell, with λz^* replaced by a dimensionless residence time in the cell.

For given kinetic parameters λ, μ, α_1, α_2, the local concentration $C^*_{B\infty}$ (and the extent of reaction of A) changes appreciably with potential, Figure 2. Thus, the potential can be used as a selectivity control variable in the kinetic regime, as with parallel reactions (Sakellaropoulos and Francis, 1979*a*, *b*).

Figures 2 and 3 show that a maximum intermediate concentration is observed ($\partial C^*_{B\infty}/\partial z^* = 0$) at an optimal reactor length z_m^*, in analogy to conventional, nonelectrochemical kinetics of series reactions

$$z_m^* = \frac{\ln\mu - (\alpha_2 - \alpha_1)\theta}{\lambda e^{-\alpha_1\theta}[\mu e^{-(\alpha_2-\alpha_1)\theta} - 1]} \qquad (14)$$

A maximum concentration of B, $C^*_{B,\max}$ corresponds to this optimal length

$$C^*_{B,\max} = \left[\frac{e^{(\alpha_2-\alpha_1)\theta}}{\mu}\right]^{\frac{\mu}{\mu - e^{(\alpha_2-\alpha_1)\theta}}} \qquad (15)$$

Table 2 presents expressions for λz_m^* and $C^*_{B,\max}$ for other kinetics. Equations (14) and (15) and those of Table 2 hold also for two consecutive reactions, of which one is a chemical step (for example, EC or CE mechanisms) with α_2 or α_1 being zero. Obviously, for two chemical steps or for $\theta = 0$, Equations (14) and (15) reduce to the expressions obtained for nonelectrochemical kinetics.

A maximum concentration $C^*_{B,\max}$ exists always for finite θ and $C^*_{Bo} = 0$. If the feed contains intermediate

TABLE 2. MAXIMUM SPACE TIME AND CONCENTRATION FOR VARIOUS KINETICS OF SERIES REACTIONS

Orders	$C^*_{B\infty}$	λz_m^*	$C^*_{B,\max}$
A. Channel flow reactor			
a. $a_{11} = b_{22} = 1$, $\mu e^{-(\alpha_2-\alpha_1)\theta} = 1$	$\lambda z^* e^{-\alpha_1\theta} e^{-\lambda z^* e^{-\alpha_1\theta}}$	$e^{-\alpha_1\theta}$	e^{-1}
b. $a_{11} = 0$; $b_{22} = 1$	$\frac{1 - \exp[-z^*\mu\lambda e^{-\alpha_2\theta}]}{\mu e^{-(\alpha_2-\alpha_1)\theta}}$	$+\infty$	$\frac{e^{(\alpha_2-\alpha_1)\theta}}{\mu}$
c. $a_{11} = 1$; $b_{22} = 0$	$1 - \mu\lambda z^* e^{-\alpha_2\theta} - e^{-\lambda z^* e^{-\alpha_1\theta}}$	$\frac{(\alpha_2-\alpha_1)\theta - \ln\mu}{e^{-\alpha_1\theta}}$	$1 + \mu e^{(\alpha_1-\alpha_2)\theta}[1 + \ln\mu - (\alpha_2-\alpha_1)\theta]$
B. Mixed reactor			
a. $a_{11} = 0$; $b_{22} = 1$	$\frac{\lambda e^{-\alpha_1\theta}}{1 + \lambda\mu e^{-\alpha_2\theta}}$	$+\infty$	$\frac{e^{(\alpha_2-\alpha_1)\theta}}{\mu}$
b. $a_{11} = 1$; $b_{22} = 0$	$\frac{\lambda}{\lambda + e^{\alpha_1\theta}} - \mu\lambda e^{-\alpha_2\theta}$	$\frac{e^{\left(\frac{\alpha_1+\alpha_2}{2}\right)\theta}}{\sqrt{\mu}} - e^{\alpha_1\theta}$	$\left\{1 - \sqrt{\mu} e^{\left(\frac{\alpha_1-\alpha_2}{2}\right)\theta}\right\}^2$

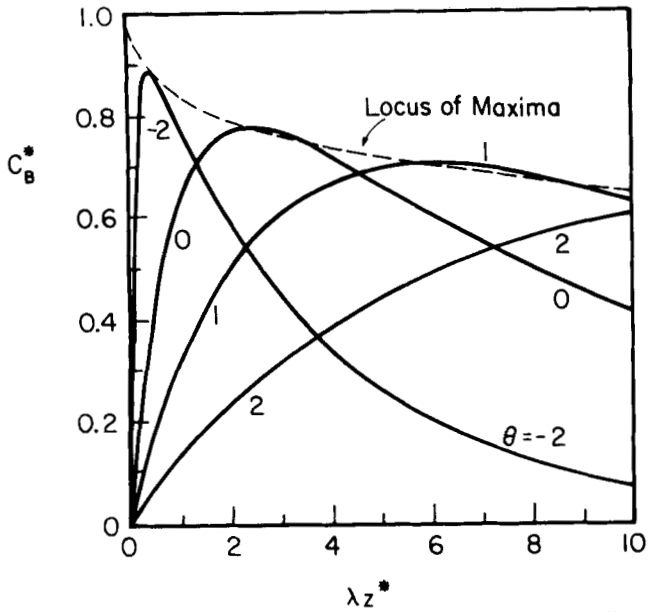

Fig. 2. Variation of the concentration of a reaction intermediate product with distance and potential in a CER. Results for a reduction with $\alpha_2 - \alpha_1 < 0$: $\alpha_1 = 1$, $\alpha_2 = 0.5$, $\mu = 0.1$.

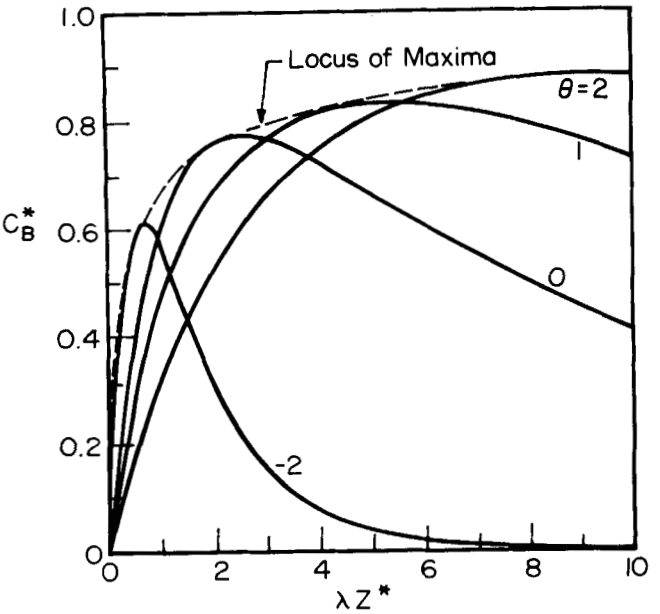

Fig. 3. Effect of potential and distance on intermediate concentration in a CER. Results for a reduction with $\alpha_2 - \alpha_1 > 0$: $\alpha_1 = 0.5$, $\alpha_2 = 1.0$, $\mu = 0.1$.

$B(C_{Bo}^* \neq 0)$, a maximum will exist only if $(\partial C_{B\infty}^*/\partial z^*)_{z^*=0} > 0$ at the reactor entrance. Although Sioda (1974) realized that a maximum yield of an intermediate is possible in electrochemical reactions, his analysis addressed only electrolysis at the limiting current. Under those conditions, reaction is mass transport limited, and no potential effects exist.

Comparison of Figures 2 and 3 with conventional plug flow reactors (Levenspiel, 1972) reveals distinct differences. The term $[\mu e^{-(\alpha_2-\alpha_1)\theta}]$ in Equations (13) and (14) does not play merely the role of a rate constant ratio as with nonelectrochemical reactions. Depending on the difference in transfer coefficients, the maximum $C_{B,\max}^*$ can be shifted to longer space times ($\alpha_2 - \alpha_1 > 0$, Figure 3) or shorter ones ($\alpha_2 - \alpha_1 < 0$, Figure 2). In the latter case, small values of $[\mu e^{-(\alpha_2-\alpha_1)\theta}]$ favor low space times or reactor volumes and high intermediate yields, in contrast to conventional kinetics. Furthermore, $C_{B\infty}^*$ does not change monotomically at a given λz^* with changing potential.

Figures 2 and 3 indicate a change in the selectivity of species B along the reactor. The local selectivity ϕ_B is defined as the ratio of the local rates, and Equations (7) and (8) yield

$$\phi_B = \frac{dC_{B\infty}^*}{-dC_{A\infty}} = 1 - \mu C_{A\infty}^{*-a11} C_{B\infty}^{*b22} e^{-(\alpha_2-\alpha_1)\theta} \quad (16)$$

The final selectivity at any length depends then on the conversion of reactant A and can be obtained from Equations (12), (13), and (16) by integrating the selectivity function (16)

$$\Phi_B = \frac{C_{B\infty}^*}{1 - C_{A\infty}^*} = \frac{\int_1^{C_{A\infty}^*} [\mu e^{-\delta\alpha\theta} C_{A\infty}^{*(\mu e^{-\delta\alpha\theta}-1)} - 1] dC_{A\infty}^*}{(\mu e^{-\delta\alpha\theta} - 1) \int_1^{C_{A\infty}^*} - dC_{A\infty}^*} \quad (17)$$

where $\delta\alpha = \alpha_2 - \alpha_1$. For the above first-order reactions

$$\Phi_B = \frac{C_{A\infty}^*}{(1 - C_{A\infty}^*)(\mu e^{-\delta\alpha\theta} - 1)} [1 - C_{A\infty}^{*(\mu e^{-\delta\alpha\theta}-1)}] \quad (18)$$

Figure 4 shows the change of selectivity with reactant concentration at various potentials. For $\mu < 1$ and $(\alpha_2 - \alpha_1)\ \theta > 0$, high reactant conversion can be obtained with small selectivity loss. The high selectivity drop with conversion for $\mu > 1$ can be partly offset by changing the potential, so that $(\alpha_2 - \alpha_1)\ \theta > 0$. This figure provides a guideline to select operating potentials and extents of reaction for selectivity control.

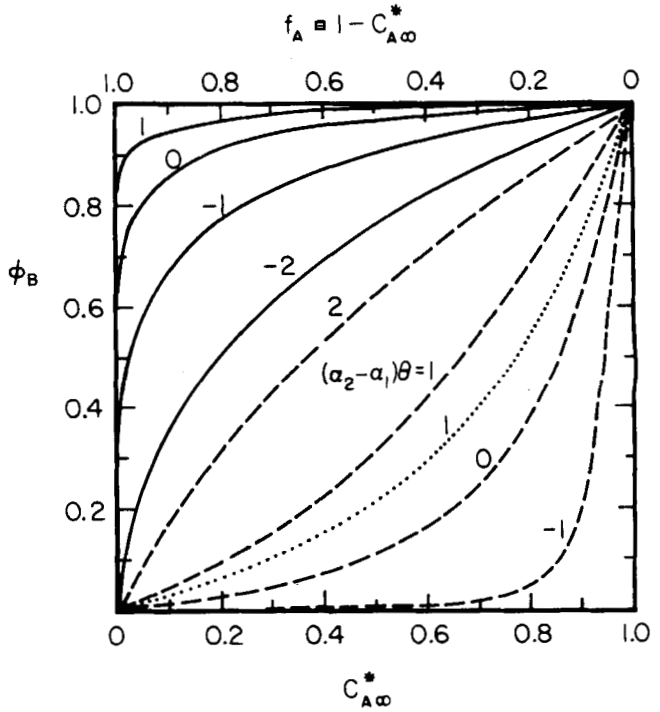

Fig. 4. Effect of reactant concentration and conversion on the selectivity of intermediate in a CER (solid and dashed curves) and in a MER (dotted curve). Solid lines: $\mu = 0.1$; dashed and dotted lines: $\mu = 10$.

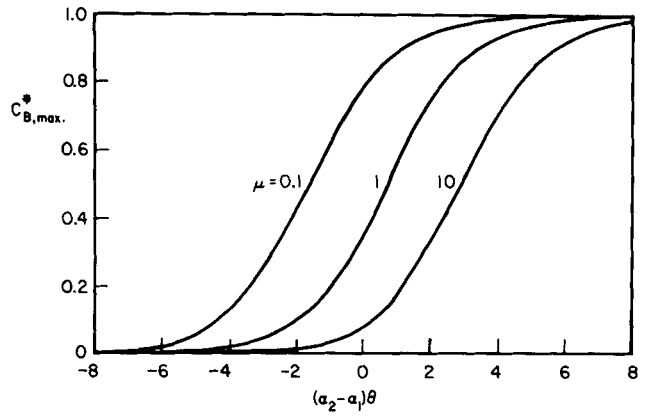

Fig. 5. Change of the intermediate maximum concentration with potential or transfer coefficient difference.

The effect of potential on selectivity and yield could be considered analogous to that of temperature. However, with Arrhenius kinetics for both reactions, an apparent activation energy difference ΔE_A^* is observed, depending on potential

$$\Delta E_A^* = (E_{A2}^* - E_{A1}^*) + (\alpha_2 - \alpha_1)\theta \qquad (19)$$

where $E_{Ak}^* = E_{Ak}/\mathcal{R}T$ are dimensionless activation energies at zero potential. An isoselective potential θ_{Is} can exist, then, if $\alpha_1 \neq \alpha_2$, for which a temperature change does not alter selectivity

$$\theta_{Is} = \frac{E_{A2}^* - E_{A1}^*}{\alpha_1 - \alpha_2} \qquad (20)$$

Equation (19) suggests that the potential can enhance, suppress, or even reverse the activation energy effect on yield. Similar behavior is also observed with parallel electrochemical reactions within a common reduction or oxidation potential range (Sakellaropoulos and Francis, 1979*b*). Figure 5 demonstrates the change in the maximum concentration of an intermediate with potential in a consecutive reaction scheme. The family of curves represents either different reactions or changes in μ due to temperature. Obviously, $C^*_{B,max}$ can be smaller or larger than that in the absence of a potential field ($\theta = 0$), depending on $[(\alpha_2 - \alpha_1)\theta]$. For a reaction sequence with $E_{A2} - E_{A1} = 10$ kcal/mole, a temperature increase of about 40°C would decrease μ by ten. Nonetheless, the attendant drop in $C^*_{B,max}$ can be offset by a very modest increase of $(\alpha_2 - \alpha_1)\theta$ by about two units.

The effect of potential on product selectivity and its temperature dependence exists, of course, only if the two reaction steps have different transfer coefficients ($\alpha_1 \neq \alpha_2$). If $\alpha_1 = \alpha_2$, Equations (12) to (19) and Table 2 still hold, but ϕ_B and $C^*_{B,max}$ are no longer functions of potential. However, the local concentrations of reactants and products and the local reaction rates still depend on the electrode potential.

Figure 5 can also be used to predict qualitatively the effect of ohmic losses in porous electrodes on product yield. For a cathodic reaction, the potential in the pores would be increasingly more positive than that at the electrode surface facing the counterelectrode. Thus, if $\alpha_1 < \alpha_2$, the concentration of species B would tend to improve in the porous electrode compared to that of a smooth one. Conversely, if $\alpha_1 > \alpha_2$, $C^*_{B,max}$ would decrease in the pores owing to the potential variation. The opposite effects are anticipated for anodic reactions. Of course, the reaction rate would not be uniform in the pores.

Optimal Yield Consideration. The current analysis indicates that optimal production of intermediate B depends on both the electrode potential and the space time (or reactor volume). From Figures 2 and 3, and for fixed reactor length and space time, a potential exists in principle that would maximize locally the yield of B. However, no finite global optimum exists for $C^*_{B\infty}$ with respect to λz^* and θ. The derivatives $\partial C^*_{B\infty}/\partial \lambda z^*$ and $\partial C^*_{B\infty}/\partial\theta$ become both zero only at the limits of $\lambda z^* \to 0$ (for $\alpha_2 - \alpha_1 < 0$) or $\lambda z^* \to \infty$ (for $\alpha_2 - \alpha_1 > 0$), where $C^*_{B,max} \to 1$.

Regardless of the values of μ and of the transfer coefficients, the reactor length for maxium B formation, when this exists, decreases sharply with decreasing potential, Figure 6. Although this would reduce the capital cost for the reactor, it may affect adversely the product yield. When $\alpha_1 > \alpha_2$, the highest intermediate yield is attained at the shortest feasible reactor length or space time and at the lowest potential, Figure 2. The system is then not amenable to operational optimization but only to economic optimization between energy costs (low potential) and reactor and chemical costs.

When $\alpha_1 < \alpha_2$, however, the yield of B decreases at low potentials, Figure 3. In this case, low conversion of reactant A per pass would be desirable to improve the yield of B (see Figure 4). Separation and recycling costs for the reactant would then figure prominently in the total process cost.

Alternatively, the selectivity and yield of B can be maximized by a variational optimization sequence, as is evident from Figure 3. This can be achieved by intentional change of the potential along the reactor, due to the change in shape and location of the curves. One can notice that decreasing potentials result in intersection of the $C^*_{B\infty} - z^*$ curves and in an increase of initial slopes $[\partial C^*_{B\infty}/\partial z^*)_{z^*=0}]$. Thus, a low potential at the reactor entrance

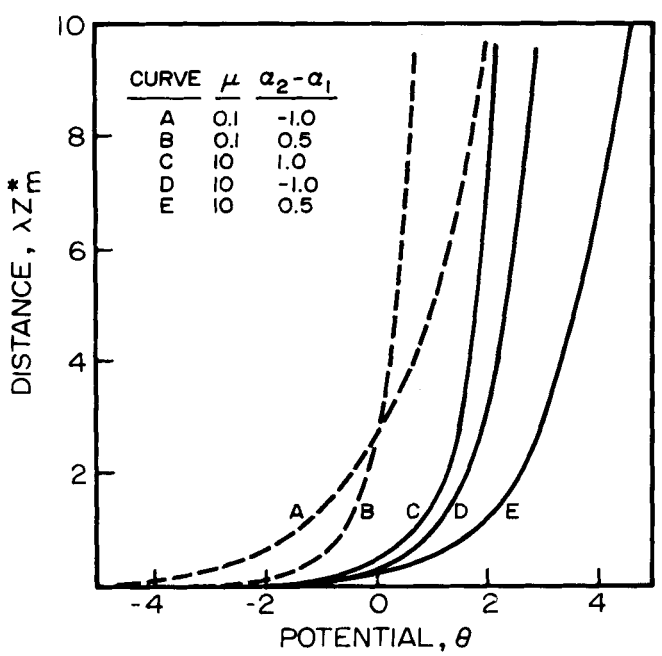

Fig. 6. Decrease of the length of a CER with potential, for maximum formation of intermediate B.

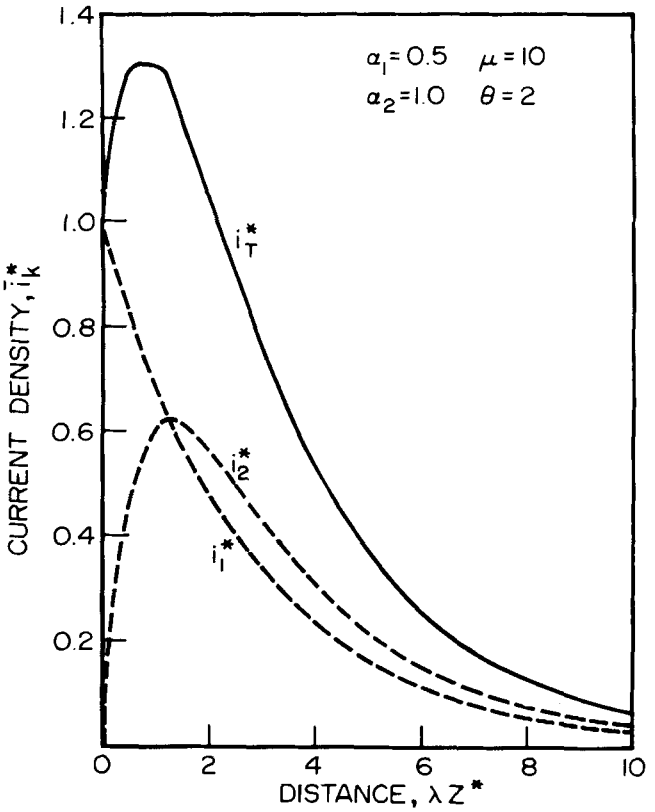

Fig. 7. Current density or rate distribution along a CER for each step (i_1^*, i_2^*) and for the overall reaction (i_t^*).

followed by a gradual increase along the locus of maxima curve would improve the yield of B at the exit, compared to simple potentiostatic operation. Such an optimal potential sequence could be attained by using sectioned working electrodes and discrete potential adjustment, or flow through electrodes with concurrent flow of reactants and of charge. In the latter, ohmic potential drop within the electrode will increase the potential at the reactor end. However, the potential sequence may not be exactly the required optimal one.

Current Distribution. Concentration variations along the working electrode of a CER lead to nonuniform local current distribution. From Equations (2), (3), (12), and (13), the local current density (rate) associated with each reaction path is estimated. For simple, first-order irreversible reductions, the local dimensionless current densities $\bar{i}_k^*(z)$ are

$$\bar{i}_1^*(z^*) = \frac{\bar{i}_1(z)}{i_o} = C_{A*}^* = \exp(-\lambda z^* e^{-\alpha_1\theta}) \qquad (21)$$

$$\bar{i}_2^*(z) = \frac{\bar{i}_2(z)}{i_o} = \frac{n_2\mu}{n_1[\mu - e^{(\alpha_2-\alpha_1)\theta}]}\{\exp(-\lambda z^* e^{-\alpha_1\theta}) - \exp(-\mu\lambda z^* e^{-\alpha_2\theta})\} \qquad (22)$$

where $\bar{i}_o$ is the local current density at the reactor inlet

$$\bar{i}_o = \sum_{k=1}^{2} \bar{i}_k(z=0) \cdot \qquad (23)$$

For $C_{Bo}^* = C_{Co}^* = 0$, $\bar{i}_o = \bar{i}_1\ (z=0)$.

A typical current distribution is shown in Figure 7 for space times that would result in maximum B formation within the reactor. While $\bar{i}_1^*$ decreases monotonically, $\bar{i}_2^*$ reaches a maximum, corresponding to z_m^*, for which the maximum concentration $C_{B,\max}$ is observed. At this point, the rates of formation and consumption of B are equal [see Equation (8)]. Depletion of C_{B*}^* at distances larger than z_m^* results in decreasing current from the second reaction. Similar behavior would be observed with oxidation reactions in series, such as hydrocarbon or alcohol oxidations.

The total, local current density $\bar{i}_t$ is given by Equation (3). In the example of Figure 7, $\bar{i}_t^*$ goes through a maximum ($\bar{i}_t^* > 1$) in the neighborhood of maximum $\bar{i}_2^*$, declining rapidly thereafter. However, a maximum in $\bar{i}_t^*$ is not expected always, even if $C_{Bo}^* = 0$ or even if $C_{B,\max}^*$ exists. A criterion for the existence of such a maximum current can be derived from the change of sign of the slope around this point. Thus, if the first derivative of $\bar{i}_t^*$ at $\lambda z^* = 0$ is zero or negative, no maximum should occur; that is

$$\left[\frac{\partial \bar{i}_t^*}{\partial(\lambda z^*)}\right]_{\lambda z^*=0} \leq 0 \qquad (24)$$

Equation (24) yields a simple quadratic equation for first-order reactions

$$\frac{n_2}{n_1}\mu^2 e^{-2\delta\alpha\theta} - \left(1 + \frac{n_2}{n_1}\right)\mu e^{-\delta\alpha\theta} + 1 \leq 0 \qquad (25)$$

For the often encountered case of $n_1 = n_2$, then, $\bar{i}_t^*$ becomes larger than unity only if

$$(\alpha_2 - \alpha_1)\theta < \ln \mu \qquad (26)$$

For the example of Figure 7, the total local current density is less than unity if $\theta > 4.6$. However, $C_{B,\max}^*$ still exists at $\lambda z_m^* > 9.97$, if $C_{Bo}^* = 0$.

If $n_1 \neq n_2$, more than one maximum can exist. With complex reactions, this implies that a step considered as single probably consists of more than one reaction in series. Therefore, the overall reaction assumed as a two-step sequence includes, in fact, more than two steps. Such behavior is discussed later for methanol oxidation. With multiple reactions of S distinct steps, $S - 1$ maxima are predicted, one for every two reaction sequences.

The position of maximum $\bar{i}_t^*$ in the reactor shifts with potential as the relative rates of the first and second step change. With increasing rate of the second reaction, the local $\bar{i}_t^*$ tends to 2 (for $n_1 = n_2$), and little intermediate is formed. In this case, the two reactions behave electrochemically as one overall reaction with a slow first step. The space time or reactor volume and potential for which this happens are important for the design of fuel cells and other electrochemical energy generation systems for maximum energy output. For an economic optimization, however, one should notice that $\bar{i}_t^*$ remains larger than unity in the reactor for lengths larger than z_m^*, Figure 7. From the sum ($\bar{i}_1^* + \bar{i}_2^*$), a criterion can be easily obtained for the length λz^* for which $\bar{i}_t^* \geq 1$, in terms of the kinetic parameter μ, α_1, α_2 and the potential θ.

Because of the nonuniform local current distribution in a CER, the average current density depends on λz^*. The average current density, defined as

$$\langle \bar{i}_t^* \rangle = \int_0^{z^*} \sum_{k=1}^{R} \bar{i}_k^* dz^* \Big/ \int_0^{z^*} dz^* \qquad (27)$$

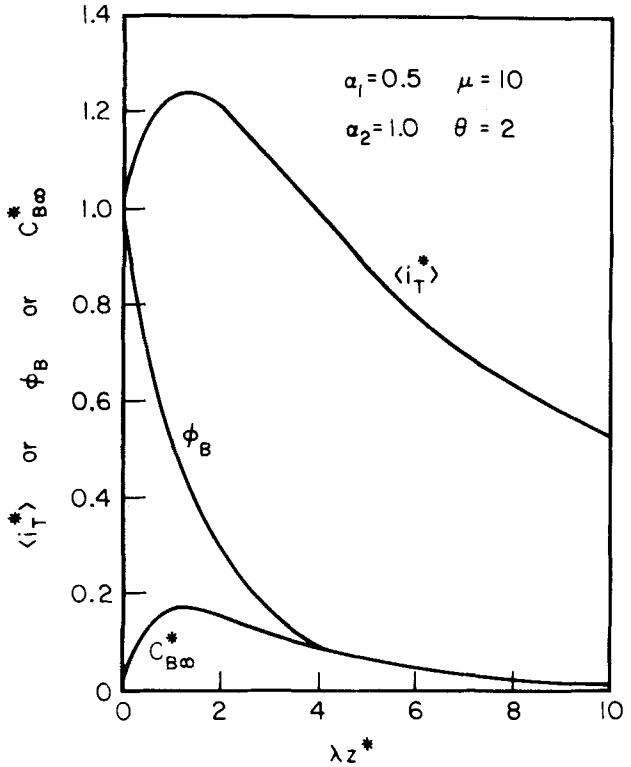

Fig. 8. Distribution of average current density and of concentration and selectivity of intermediate B in a CER for the results of Figure 7.

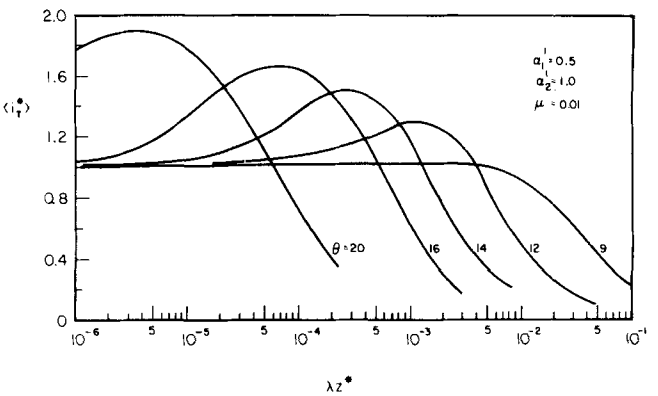

Fig. 9. Variation of the average current density of a CER with potential and distance for an oxidation series reaction.

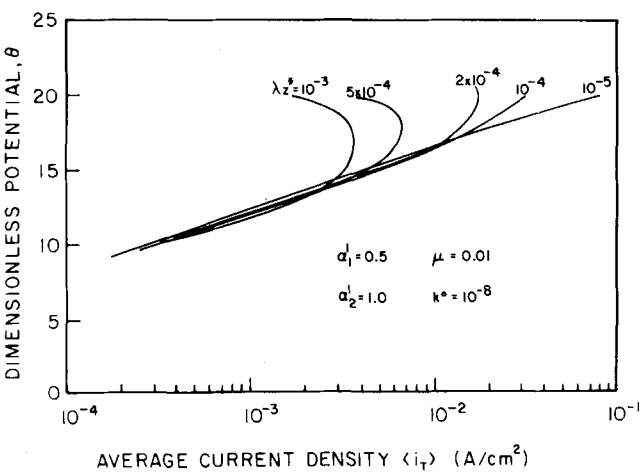

Fig. 10. Potential average current density behavior of a CER at various lengths or space times for the oxidation reaction of Figure 9: $C_{Ao} = 10^{-3}$ mole/cm^3.

is associated with the overall energy requirements of the reactor or the electric energy generation capabilities for electrogenerative systems. From the discussion above, it becomes obvious that the energy capabilities of an electrogenerative reaction are minimal for high yields of the intermediate per pass.

In Figure 8, the average current density is shown in relation to the concentration of intermediate B and the overall selectivity ϕ_B for the parameters used in Figure 7. The change of $\langle \bar{i}_t^* \rangle$ with λz^* is more uniform than the local $\bar{i}_t^*$ variation, Figure 7. Of course, the average current and energy for various space times would change with potential. Figure 9 exemplifies this behavior for an irreversible oxidation reaction with a relatively slow second step. This system is quite typical of the electrocatalytic oxidation of hydrocarbons and alcohols in fuel cells (Vielstich, 1970) or of selective oxidations to aldehydes (Goodridge and King, 1970).

In this scheme, a maximum $\bar{i}_t^*$ is observed for $\theta > 9.2$ [Equation (26)]. The second reaction rate increases here with increasing potential, while the selectivity for intermediate formation decreases. The average current density becomes flatter and is shifted to lower space times with increasing rate (see also Figure 3 for a reduction). The results of Figure 9 hold for $\alpha_1 < \alpha_2$. If $\alpha_1 > \alpha_2$, the equivalent curves would shift to higher space times with increasing potential. Although results are presented for a small μ, similar behavior would be observed for $\mu > 1$, with the curves shifted to even lower space times.

Figure 9 has important implications for the design of flow cells for electrochemical energy generation. At fixed potential, the maximum energy or current capability is not achieved for nearly complete conversion of reactant and intermediate per pass. The declining concentrations of A and B drastically reduce the average current in this case [Equation (8)]; thus, increasing the reactor length or the space time would be detrimental to energy output. From the shape and shifting of the curves of Figure 9, it becomes obvious, then, that a change in space time is necessary to accompany any potential change for both selectivity and energy output control. Similar considerations can be extended to energy consumption with conventional electrochemical reactors. In the latter case, however, a maximum current is associated with maximum energy consumption.

Energy output or consumption evaluations are usually based upon the actual potential current density behavior of the reactor. In Figure 10, the anticipated average current densities with potential were calculated at various λz^* for the parameter values of Figure 9 [Equation (21) to (23)]. At low space times or short reactors ($\lambda z^* = 10^{-5}$), a virtually Tafel (semilogarithmic) behavior is predicted, despite the presence of two simultaneous reactions. At long retention times, however, an unusual decrease of the current density occurs with increasing potential beyond a certain value. Such behavior arises from the fast depletion of reactants A and B in the reactor at high potentials (see Figure 9).

Potential current density curves similar to those of Figure 10 have been observed experimentally in the electrooxidation of unsaturated hydrocarbons on platinum electrodes (Bockris et al., 1965; Johnson et al., 1970), and in the emulsion oxidation of benzhydrol (Franklin and Sidarous, 1977). However, such maxima currents have usually been attributed to electrode passivation (Bockris et al., 1965). The results of Figure 10 indicate that incidental choice of space times (or residence

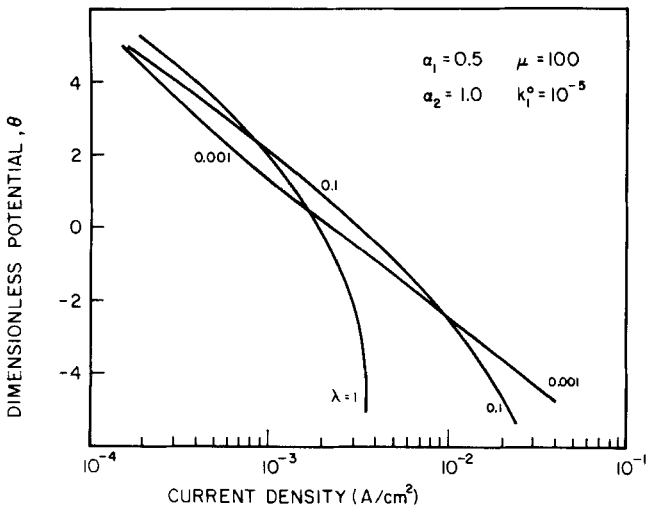

Fig. 11. Potential current density behavior of a MER for two consecutive reductions; $C_{Ao} = 10^{-3}$ mole/cm³.

times in batch cells) can also yield apparent limiting currents with consecutive reactions. It should be noticed that at low potentials a nearly Tafel behavior is observed for all space times. From the slope $[2.3RT/\alpha_1'F]$, an apparent transfer coefficient $\alpha_1' \simeq 0.44$ can be calculated which is close to the transfer coefficient of the first reaction ($\alpha_1' = 0.5$). This apparent Tafel slope and possible cursory product analysis could be misinterpreted as the result of one main reaction, that of the first oxidation step.

Mixed Electrochemical Reactors

Presently, few multiple electroorganic reactions have been well characterized in their kinetic regime. With arbitrary, unknown kinetics, analysis of such reactions in a batch cell or a CER becomes cumbersome, requiring solution and testing of the often nonlinear differential Equations (7), (8), and (10). A MER in this case would simplify kinetic and selectivity investigation. Therefore, we will discuss briefly the selectivity response of this reactor.

With consecutive reactions (6), the convective transport equation for a MER, Equation (5), gives

$$C_{A\infty}^* + \lambda C_{A\infty}^{*a11}\, e^{-\alpha_1\theta} = 1 \tag{28}$$

$$C_{B\infty}^* - \lambda C_{A\infty}^{*a11}\, e^{-\alpha_1\theta}\,[1 - \mu C_{A\infty}^{*-a11}\, C_{B\infty}^{*b22}\, e^{-(\alpha_2-\alpha_1\theta)}] = 0 \tag{29}$$

Equations (28) and (29) can be solved easily for some simple reaction orders (0, 1), Table 2. With orders of 0.5 or 2, the resulting quadratic equations do not take a simple form. However, even with more complex kinetics, computational analysis is simpler than solution of Equations (7) and (8).

For the simplest case of two first-order reactions in series, the concentrations depend on space time λ and potential θ:

$$C_{A\infty}^* = \frac{1}{1 + \lambda e^{-\alpha_1\theta}} \tag{30}$$

$$C_{B\infty}^* = \frac{\lambda e^{-\alpha_1\theta}}{(1 + \lambda e^{-\alpha_1\theta})(1 + \lambda\mu e^{-\alpha_2\theta})} \tag{31}$$

A maximum $C_{B,\max}^*$ is then expected at $\lambda_m\left(\frac{\partial C_{B\infty}^*}{\partial\lambda} = 0\right)$:

$$\lambda_m = \frac{1}{\sqrt{\mu}} \exp\left(\frac{\alpha_2 + \alpha_1}{2}\theta\right) \tag{32}$$

$$C_{B,\max}^* = 1 \Big/ \left\{1 + \sqrt{\mu}\exp\left[-\left(\frac{\alpha_2 - \alpha_1}{2}\right)\theta\right]\right\}^2 \tag{33}$$

Therefore, $C_{B\infty}^*$ will vary with λ and θ in a fashion similar to Figures 2 and 3, but the yield of intermediate will always be lower in a MER. This is demonstrated in Figure 4 by comparing the selectivity of B at any conversion for a MER and a CER (curves for $\theta = 1$, $\mu = 10$). Here the selectivity is uniform throughout the reactor

$$\Phi_B = \frac{C_{B\infty}^*}{1 - C_{A\infty}^*} = \frac{1}{1 + \mu\lambda\exp[-(\alpha_2 - \alpha_1)\theta]}$$

$$= 1 - \left(\frac{n_1}{n_2}\right)\left(\frac{\bar{i}_2^*}{\bar{i}_1^*}\right) \tag{34}$$

where λ is a function of the reactant concentration $C_{A\infty}^*$, Equation (30). Similar expressions can, of course, be derived for other rate expressions.

The contribution of each reaction step to the reactor current density can be calculated from Equations (2), (3), (30) and (31):

$$\bar{i}_1^* = \frac{\bar{i}_1}{\bar{i}_0} = \frac{1}{1 + \lambda e^{-\alpha_1\theta}} \tag{34a}$$

$$\bar{i}_2^* = \frac{\lambda\mu e^{-\alpha_2\theta}}{(1 + \lambda e^{-\alpha_1\theta})(1 + \lambda\mu e^{-\alpha_2\theta})} \tag{35}$$

$$\bar{i}_t^* = \frac{1 + 2\lambda\mu e^{-\alpha_2\theta}}{(1 + \lambda e^{-\alpha_1\theta})(1 + \lambda\mu e^{-\alpha_2\theta})} \tag{36}$$

where $\bar{i}_0 = \sum_R \bar{i}_k$, evaluated at the inlet concentrations. In all cases, $\bar{i}_2^* \leq \bar{i}_1^*$, so that Φ_B remains always positive.

The total current density of a MER is uniform, but it depends on space time and extent of reaction, Equations (34) to (36). However, an $\bar{i}_t^* > 1$ is expected if $\mu \geq 1$, for which $(\partial\bar{i}_t/\partial\lambda)_{\lambda=0} \geq 0$. The variation of the total current density with space time λ is similar to that of Figure 9 for a CER, discussed earlier. Thus, depletion of both A and B at high values of dimensionless space time results in potential current density curves that approach an apparent limiting current, Figure 11, as with a CER (Figure 10). Again, an apparent transfer coefficient can be calculated from Figure 11 at low current densities, with a value close to that of α_1. The trends discussed here for first-order reactions also apply to other rate equations.

For the same kinetic parameters, potential and space time, the total current density of a MER is generally lower than that of a CER, despite the higher selectivity of the MER for final product C. This results from the lower extent of reaction in this reactor compared to a CER of similar space time. Therefore, the capital expenditures for a MER or its energy output will be inferior to a channel flow cell. However, uniform current density, concentration, and selectivity make a MER suitable for specificity analyses of multiple reactions.

Some Examples of Selectivity Analysis

Equations (28) and (29) are the basis for kinetic and selectivity investigations of multiple reaction sequences.

In particular, determination of the transfer coefficient of each step is essential to understand the effect of the electrode potential. Experimental results of $C^*_{A\infty}$, $C^*_{B\infty}$ at various potentials in a MER yield $(\alpha_2 - \alpha_1)$ and μ, using Equation (37):

$$1 - \Phi_B = \Phi_C = \mu \left(\frac{C^{*b_{22}}_{B\infty}}{C^{*a_{11}}_{A\infty}} \right) \exp\left[-(\alpha_2 - \alpha_1)\theta\right] \tag{37}$$

In Figure 12 we made use of previously published results on the electrogenerative reduction of gaseous vinyl fluoride on platinum-black in a MER (Sakellaropoulos and Langer, 1976*b*) to show that a semilogarithmic relation holds for Φ_C and θ. In this reaction, cleavage of the fluorine atom is followed by electroreduction of intermediate ethylene to ethane. Φ_C is the gas-phase selectivity of ethane, and all reactants and products are assumed in equilibrium with the electrolyte.

From Figure 12 we obtain $\alpha_2 - \alpha_1 = 0.52$ and $k^o_2/k^o_1 = 6.9$. These results and known parameters ($\alpha_2 = 1.7$, $k^o_2 = 3.2 \times 10^{-3}$ mole/cm^2·s) for the second reaction step, the ethylene reduction (Langer and Sakellaropoulos, 1975), permit evaluation of α_1, k^o_1. We wish to note, however, that vinyl fluoride reduction may have been influenced by slow reactant transport in the electrode pores. If k^o_2, α_2 are not known, kinetic information ($C^*_{A\infty}$ vs. λ) at low reactant conversions would yield k^o_1, α_1 independently, using Equation (28).

The above results were obtained with thin porous electrocatalysts (~ 0.01 cm) at total current densities ≤ 0.025 A/cm^2. With an electrolyte conductivity of 0.74 Ohm^{-1} cm^{-1} and assuming a typical electrode porosity and tortuosity of 0.4 and 5, respectively, ohmic losses in the pores are estimated to be ~ 0.006 V. Thus, the assumption of negligible potential variation in the pores is justified, compared with the actual potential of 0.1 to 0.2 V, Figure 12, at the electrode surface.

Rate constants and transfer coefficients of simple-order reactions can be also obtained from concentration-residence time data at constant potential in a CER or a batch cell. For example, Vielstich (1970) reports such data for a closed cell electrooxidation of methanol on planar platinum in alkaline electrolytes:

$$CH_3OH \xrightarrow{-4e} HCOO^- \xrightarrow{-2e} CO_3^{2-} \tag{38}$$

The concentration of $HCOO^-$ reaches a maximum at about 2.75 time units. At this maximum, $dC_B^*/dt^* = 0$, and for $\lambda z^* = t^*$ in a closed cell, Equation (8) yields, assuming first-order reactions

$$\frac{k_2^o}{k_1^o} \exp\left[-(\alpha_2 - \alpha_1)\theta\right] = \frac{C_A^*}{C_B^*} = 0.47 \tag{39}$$

From $C_A - t$ data (Vielstich, 1970), we can also calculate $k_1^o \exp(-\alpha_1\theta)$, using Equation (7). The initial slope $(dC_A/dt)_{t=0}$ at $C_A = C_{Ao} = 0.75$ mole/l gives $k_1^o \exp(-\alpha_1\theta) \simeq 0.33$ h^{-1}. This and Equation (39) yield $k_2^o \exp(-\alpha_2\theta) \simeq 0.15$ h^{-1}. These results are in agreement with the suggested relationship $k_2 < k_1$ (Vielstich, 1970). Although this is true at one potential, selectivity potential information is necessary to determine whether $\mu < 1$. Obviously, the values of $(\alpha_2 - \alpha_1)$ and k_2^o/k_1^o are needed to predict the maximum yield at other potentials, Equation (15).

The results obtained here can be used to design a CER for methanol oxidation only at the potential at which they were reported. If formate ions were the desired product, their maximum concentration would be that of the $C_{B,\max}$ in the closed cell. This would be attained at a space time equivalent to the maximum residence time in the batch reaction [Equations (14) and (15)].

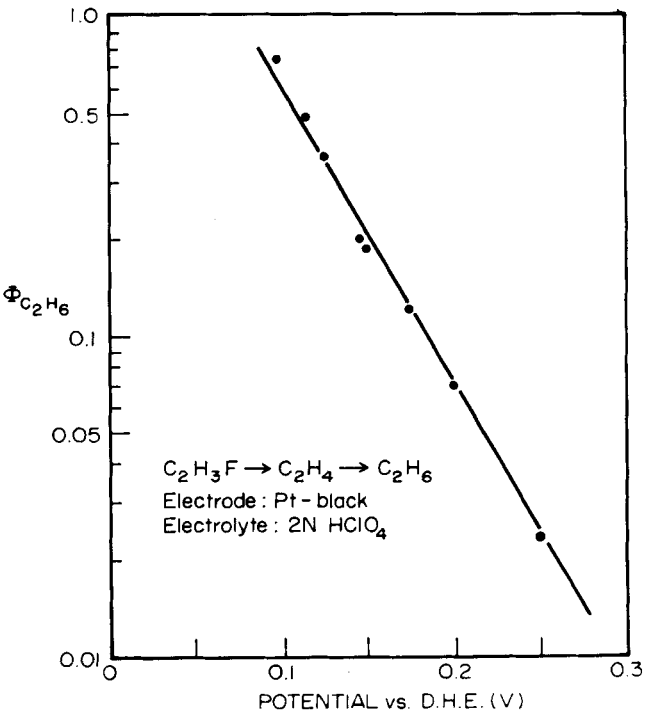

Fig. 12. Effect of electrode potential on the final product selectivity of a series reaction. Electrogenerative reduction of vinyl fluoride on platinum at 25°C (Sakellaropoulos and Langer, 1976b). Cathode potential is referenced here with respect to the dynamic hydrogen electrode (DHE) in 2N $HClO_4$. ($E°_{H_2,DHE} \simeq 0.018$ V vs. NHE).

Methanol oxidation is, however, considered for fuel cell electrochemical energy generation. Prediction of the current density distribution and output would require a detailed knowledge of the electrode kinetics of each reaction. This is usually obtained by studying the individual reactions (Vielstich, 1970) and is beyond the scope of the present discussion. However, it is important to note that Equation (25) suggests the existence of two maxima for the total current density distribution, corresponding to $\mu\exp\left[-(\alpha_2 - \alpha_1)\theta\right] > 2$ and > 1. The latter maximum arises from the stepwise oxidation of methanol to formate via a formaldehyde intermediate. Thus, reaction (38) is, in fact, a three-step sequence. Stationary (closed cell) potential current density data have yielded two current maxima in some occasions, and formaldehyde has been identified as a product (Vielstich, 1970). In the results of Equation (39), product analysis was obtained at a potential away from either of the two current maxima.

From these examples, it becomes obvious that a selectivity analysis over a wide potential range could help explain experimental results and would assist in reactor design and optimization. Unfortunately, such information is scanty at present in the electrochemical literature.

ACKNOWLEDGMENT

The author wishes to thank Rensselaer Polytechnic Institute for partial support of this work.

NOTATION

A_j = reactant or product species j
a_{kj} = reaction order of A_j in the forward reaction

b_{kj} = reaction order of A_j in the reverse reaction
C_j = concentration of species A_j (mole/cm^3)
DHE = dynamic hydrogen electrode
D_c = characteristic diameter
D_j = diffusivity of j (cm^2/s)
E = electrode potential vs. a standard reference (V)
E_A = activation energy of a reaction step (J/mole)
F = Faraday's constant (A·s/equiv)
f_j = conversion of species j
$\bar{i}$ = local current density for reaction k (A/cm^2)
$\bar{i}_t^*$ = total current density (A/cm^2)
$<\bar{i}>$ = average current density (A/cm^2)
j = all S reactants and products, ionic or molecular
k = R independent reaction paths
K_H = Henry's constant (mole/cm^3 atm)
K_j = adsorption constants for species j
k_k^o = rate constant of the k^{th} reaction at zero potential (mole$^{1-a_{kj}}$ cm$^{3a_{kj}-2}$·s^{-1})
L = reactor or electrode length (cm)
m, p = exponents in rate Equation (2)
NHE = normal hydrogen electrode
n_k = number of electrons exchanged in the k^{th} reaction
R = number of independent reactions
$\mathcal{R}$ = universal gas constant (J/mole °K)
$\bar{r}_k$ = net local, surface rate of reaction k (mole/cm^2·s)
S = total number of reactive species
S_g = catalyst or electrode specific area per unit mass (cm^2/g)
T = temperature (°K)
$\bar{v}$ = velocity of reacting fluid in the reactor (cm/s)
z = length along the electrode (cm)

Greek Letters

α_k, α'_k = transfer coefficients in the k^{th} reaction
ϵ = voidage of the control volume
$\delta\alpha$ = difference in transfer coefficients ($= \alpha_2 - \alpha_1$)
θ = dimensionless potential ($= EF/RT$)
λ = dimensionless space time $[= \rho_b S_g (1-\epsilon) k_1^o \tau\, C_{Ao}{}^{a-1}]$
μ = dimensionless selectivity parameter at zero potential ($= k_2^o C_{Ao}{}^{b_{22}-a_{11}}/k_1^o$)
ν_{kj} = stoichiometric coefficient of species A_j
ρ_b = catalyst bulk density (g/cm^3)
τ = space time ($= L/\bar{v}_z$), (s)
Φ_j = selectivity of species j, Equation (17)

Subscripts

A = reactant A
b = backward reaction
f = forward reaction
j = reactive species
k = reaction number
m = position of maximum intermediate concentration
o = initial value, at inlet conditions
1, 2 = reaction numbers to which quantities refer
∞ = local bulk properties and rates

Superscripts

o = value at zero electrode potential vs. NHE
$*$ = dimensionless quantity

LITERATURE CITED

Alkire, R., and R. Gould, "Analysis of Multiple Reaction Sequences in Flow-Through Porous Electrodes," *J. Electrochem. Soc.*, **123**, 1842 (1976).

Ateya, B. G., and L. G. Austin, "Steady-State Polarization at Porous, Flow-Through Electrodes with Small Pore Diameter," *ibid.*, **124**, 1540 (1977).

Austin, L. G., "Fuel Cells," *NASA SP-120*, pp. 310, 313, Washington, D.C. (1967).

Bard, A. J., and J. S. Mayell, "Secondary Reactions in Controlled Potential Coulometry," *J. Phys. Chem.*, **66**, 2173 (1962).

Bockris, J. O'M., and S. Srinivasan, *Fuel Cells, Their Electrochemistry*, p. 97, McGraw-Hill, New York (1969).

Bockris, J. O'M., H. Wroblowa, E. Gileadi, and B. J. Piersma, "Anodic Oxidation of Unsaturated Hydrocarbons on Platinized Electrodes," *Trans. Faraday Soc.*, **61**, 2531 (1965).

Fitzjohn, J. L., "Electroorganic Synthesis," *Chem. Eng. Progr.*, **71**, 85 (1975).

Franklin, T. C., and L. Sidarous, "The Effect of Surfactants on the Electrooxidation of Benzhydrol in Emulsion and Micelle Systems," *J. Electrochem. Soc.*, **124**, 65 (1977).

Geske, D. H., and A. J. Bard, "Evaluation of the Effect of Secondary Reactions in Controlled Potential Coulometry," *J. Phys. Chem.*, **63**, 1057 (1959).

Gileadi, E., and S. Srinivasan, "Electrochemical Kinetics of Parallel Reactions," *J. Electroanal. Chem.*, **7**, 452 (1964).

Goodridge, F., and C. J. H. King, "Oxidation of Ethylene at a Palladium Electrode," *Trans. Faraday Soc.*, **66**, 2889 (1970).

Ibl, N., and A. Selvig, "Electrosynthese von Aethylen- und Propylen-chlorhydrin," *Chem.-Ing. Techn.*, **42**, 180 (1970).

Johnson, J. W., S. C. Lai, and W. J. James, "Anodic Oxidation of Ethylene on Gold Electrodes," *Electrochim. Acta.*, **15**, 1511 (1970).

Kramers, H., and K. R. Westerterp, *Elements of Chemical Reactor Design and Operation*, Netherlands Univ. Press, Amsterdam (1963).

Langer, S. H., and H. P. Landi, "Electrogenerative Hydrogenation," *J. Am. Chem. Soc.*, **85**, 3043 (1963).

Langer, S. H., and G. P. Sakellaropoulos, "Kinetics of Electrogenerative Hydrogenation over Platinum Black Electrocatalyst," *J. Electrochem. Soc.*, **122**, 1619 (1975).

Levenspiel, O., *Chemical Reaction Engineering*, p. 177, J. Wiley, New York (1972).

McIntyre, J. D. E., "On the Distinction Between the Kinetics of Parallel and Heterogeneous Catalytic Electrode Reactions," *J. Phys. Chem.*, **73**, 4111 (1969).

Newman, J., and W. Tiedemann, "Porous-Electrode Theory with Battery Applications," *AIChE J.*, **21**, 25 (1975).

Parsons, R., "Effect of Electrode Material on the Product of Branched Electrochemical Reactions," *Disc. Faraday Soc.*, **45**, 40 (1968).

Pickett, D. J., *Electrochemical Reactor Design*, Elsevier, Amsterdam (1977).

Pshenichnikov, A. G., A. A. Michri, and M. Y. Kats," Electrooxidation of Ethylene at a Porous Electrode; I. Theoretical Calculation," *Elektrokhim.*, **8**, 889 (1972).

Sakellaropoulos, G. P., "A Simple Model for Intraelectrode Mass Transport and Reaction in Porous Catalytic Electrodes," 28 Int. Soc. Electrochem. Meeting, *Electrochemical Power Sources*, **2**, 290 (1977).

———, and G. A. Francis, "Selectivity and Reactor Analysis for Parallel Electrochemical Reactions," Symposium on Electrochemical Reaction Engineering, Southampton, England (Apr. 18-20, 1979*a*).

———, "Electrochemical Reactor Analysis; Selectivity of Multiple Competing Reactions," *J. Electrochem. Soc.* (1979*b*).

Sakellaropoulos, G. P., and S. H. Langer, "The Role of Electrogenerative Processing in Environmental Protection and Energy Conservation," *Trans. Am. Nuclear Soc.*, **23**, Suppl. 1, 23 (1976*a*).

———, "Electrocatalysis; Selective Electrogenerative Reduction of Organic Halides," *J. Catalysis*, **44**, 25 (1976*b*).

———, "Mass Transport Processes at Porous Electrocatalysts in the Electrogenerative Reactor," *J. Electrochem. Soc.*, **124**, 1548 (1977).

———, "Reaction Kinetics in Porous Electrocatalysts," *AIChE J.*, **24**, 1115 (1978).

Sioda, R. E., "Certain Parameter Aspects of the Flow Electrolysis on Porous Electrodes," *Electrochim. Acta.*, **19**, 57 (1974).

Trainham, J. A., and J. Newman, "A Flow-through Porous Electrode Model: Application to Metal-Ion Removal from Dilute Streams," *J. Electrochem. Soc.*, **124**, 1528 (1977).

Vielstich, W., *Fuel Cells*, D. J. G. Ives, trans., p. 88, Wiley-Interscience, New York (1970).

Weinberg, N. L., "Candidate Electroorganic Processes," paper presented at 84 National AIChE Meeting, Atlanta, Ga. (Feb. 27, 1968).

White, R., and J. Newman, "Simultaneous Reactions on Rotating-Disk Electrodes," *J. Electroanal. Chem. Interfacial Electrochem.*, **82**, 173 (1977).

White, R., J. A. Trainham, J. Newman, and T. W. Chapman, "Potential Selective Deposition of Copper from Chloride Solutions Containing Iron," *J. Electrochem. Soc.*, **124**, 669 (1977).

Manuscript received November 14, 1978; revision received March 26, and accepted April 18, 1979.

Absorption of Carbon Dioxide into Aqueous Monoethanolamine Solutions

HARUO HIKITA
SATORU ASAI
YOSHIO KATSU
and
SEIICHI IKUNO

Department of Chemical Engineering
University of Osaka Prefecture
Sakai, Osaka, Japan

The rates of absorption of pure carbon dioxide into aqueous monoethanolamine solutions with a surface active agent were measured at 15°, 25°, 35°, and 45°C in a liquid jet column and a wetted wall column. Experimental results were analyzed with the chemical absorption theory based on the penetration model. Physical solubility of carbon dioxide in aqueous monoethanolamine solutions was determined from the absorption rates measured in a near pseudo first-order reaction regime and was shown to be considerably larger than the physical solubility in water. The measured absorption rates were in good agreement with the theoretical predictions for gas absorption with an irreversible second-order reaction, when the variation of the physical solubility of carbon dioxide due to the change in the composition of the solution during the absorption process was taken into account.

SCOPE

The absorption of carbon dioxide from gas mixtures by aqueous monoethanolamine solutions is an important industrial process. Despite a considerable number of studies, severe disagreements exist between the previous experimental data on the absorption rate of carbon dioxide into aqueous monoethanolamine solutions and the theoretical predictions. These disagreements are attributed partly to interfacial turbulence due to Marangoni instability as suggested by Brian et al. (1967). They showed that the use of the physical mass transfer coefficient measured under conditions where the interfacial turbulence was present resulted in a considerable improvement in the agreement between the experimental data on the absorption rate of carbon dioxide into aqueous monoethanolamine solutions in a short wetted wall column and the chemical absorption theory based on the penetration model. However, it appears that this agreement is not satisfactory. Recently, Sada et al. (1976, 1977*b*) have measured the absorption rate of carbon dioxide into aqueous monoethanolamine solutions in laminar liquid jet and wetted wall column absorbers under conditions where the interfacial turbulence was suppressed by adding trace amounts of surface active agent to the solutions and concluded that the measured absorption rates were in good agreement with the theoretical predictions based on the penetration model. However, the value of the rate constant of the reaction between carbon dioxide and monoethanolamine, employed for the analysis of the experimental results, was obtained from the absorption rate data taken under pseudo first-order reaction conditions and is considerably higher than that obtained by the conventional kinetic method.

The purposes of the study described here are to obtain reliable data on the absorption rate of carbon dioxide into aqueous uncarbonated and partly carbonated monoethanolamine solutions under the conditions of no interfacial turbulence and to clarify the kinetics of chemical absorption for the present system.

Correspondence concerning this paper should be addressed to Haruo Hikita.

0001-1541-79-2745-0793-$00.95.